American Journal of Chemical Engineering
2022; 10(5): 89-102
http://www.sciencepublishinggroup.com/j/ajche
doi: 10.11648/j.ajche.20221005.11
ISSN: 2330-8605 (Print); ISSN: 2330-8613 (Online)

Experimental and Modeling Investigation of Heat and Mass Transfers in an Airlift Packed Column Humidifier

Adel Oueslati[1, 2]

[1]Process Engineering Department, Higher Technological Studies Institute of Zaghouan, Mogren, Tunisia

[2]Applied Mineral Chemistry Laboratory (LCMA) LR19ES02, Faculty of Science, Tunis El Manar University, Tunis, Tunisia

Email address:
adel.oueslati@isetkh.rnu.tn, waslatiad@gmail.com

To cite this article:
Adel Oueslati. Experimental and Modeling Investigation of Heat and Mass Transfers in an Airlift Packed Column Humidifier. *American Journal of Chemical Engineering*. Vol. 10, No. 5, 2022, pp. 89-102. doi: 10.11648/j.ajche.20221005.11

Received: July 22, 2022; **Accepted**: August 25, 2022; **Published**: September 21, 2022

Abstract: Background: the use of air humidification in order to produce pure water from saline or waste water take more and more importance since it allows to add value to non-pure water. In this case, the aim of this study was to simulate of air humidification. Material Methods: The experimental device used, for the humidification of the air through its contact with water, is a vertical column filled with packing. It works on the principle of an air lift pump. Modeling equations for heat and material transfer between fluids have been established. Results: Established models are verified by experimental results. The humidification of the air is proportional to the operating parameters such as: the initial level of water in the column, the air flow, the temperature of the liquid and the height of contact between fluids. The air temperature and humidity profiles increase as a function of the packing height. Conclusion: Air humidification is effective if heat and mass transfers between fluids are high. The temperature of the liquid water has a greater effect than those of the other operating parameters on the shape of the air temperature and humidity profiles as a function of the height of the column.

Keywords: Humidification-Dehumidification, Airlift Pump, Temperature Profile, Humidity Profile, Column Height, Efficiency

1. Introduction

Humidification-dehumidification desalination (HDD) is considered as one of many techniques used for the production of distilled water for small to medium-sized units. The cost of desalination depends mainly on the investment and the energy source used such as renewable energy or waste energy. Several configurations are tested under various operating conditions. Note that the HDD and the cooling towers are air-water contactors but with different objectives even if they have the same configuration and operated under the same operating conditions.

Water desalination by humidification dehumidification has been the subject of many papers. He weifeng [1] studied the effects of layouts on the performance of HDD systems. For a packed column humidifier, he concluded that the humidifier volume is to the air and water flow rates. However, this volume can be minimum when the mass transfer coefficient and the exchange area are great.

Fissal Abdel-Hady [2] presented experimentally investigate the principal operating parameters of a humidifier of small diameter and small height. This small equipment of HDD consists of several packing beds separated by an empty space. The packing particles used have a cylindrical shape with several heights and several diameters of 8mm. The main operating conditions studied were the water and air flow rates, water temperature. The experimental work led to the conclusion that productivity is favored by the increase in air flow and water temperature. However, performance decreases if the water-air flow rate ratio (mw/ma)> 1.

Adel Ben Lakhdhar Oueslati [3] suggested a packed column evaporator of heated water in counter current flow with air. A transient analysis has been carried out since the system uses solar energy to heat water in appropriate collectors. The profiles of water and air temperatures as well as absolute humidity are plotted against time. Air humidity has been shown to be highest when water and air temperatures are simultaneously high. The negative effect of the ratio increase (mw/ma) on the performance of the

humidifier has been confirmed.

Xinvi Zhou and Alsehi [4, 5] carried out a digital then experimental investigation on an HDD system where water is heated using any energy source, then sprayed in an ascending air flow. A modeling of the system was set up based on the conservation equations of mass and energy in the humidifier. The experimental results confirmed the validity of the established model. The performances of the humidifier are maximum for a flow rate ratio (mw/ma) equal to 1. Beyond this value, the performances decrease. These results are confirmed by Xin Huang [6] using another humidification system based on the spraying of hot water into the air.

TM Khass suggested HDD system with a vertical packed column humidifier in which a falling heated water in counter current flow with air [7]. Several types of packing have been tested. The results obtained show that the humidity of the air increases with the increase in temperature and water flow rate in the humidifier for all types of packing and for natural and forced flows of fluids. The same study has shown experimentally that the humidification of the air and the heat exchange between fluids are very high when the flow of fluids is forced and unnatural.

Other studies of the profiles of water and air temperatures versus a packed column volume of a cooling tower have been carried out by A. Zargar [8]. The results of these studies showed that the dry air temperature and absolute humidity increase with the increase of the packed column volume crossed by the air for an optimal ratio of water-air flow rates. As a consequence, the potential for evaporation and heat exchange between fluids increases with the increase in packing volume. These results are confirmed by ACB Thomé [9] using another configuration of cooling towers with structured packing and not in bulk.

A review of the open literature shows that heat and mass transfers depend on several parameters such as: water temperature, air and liquid flow rates ratio, type and height of packed column. For counter-current systems [1-9], the temperature and humidity of the air at the outlet of the humidifier also depend on the ratio of the water-air flow rates (mw/ma). If (mw/ma $\leq$1) then the humidification is optimal. Otherwise (mw/ma $\geq$1) then the humidification decreases which is explained by the increase in the pressure on the air by a large flow of water. Beyond a certain ratio value (mw/ma), the air flow will be slowed down by a clogging phenomenon which constitutes an unfavorable condition for the evaporation of water. For humidification systems with almost stagnant water, the air humidity at the outlet of the humidifier reaches a value greater than 0.8 kg of water/kg of dry air by ES El Agouz [10], Z. Rahimi Ahar [11] and Mohamed ASA [12]. Indeed, for a stagnant liquid crossed by air bubbles, the humidification depends on the duration of contact between hot water and air. That is to say, it depends on the speed of the air and the thickness of the water layer.

For down flow systems, the temperature and humidity of the air leaving the humidifier are not sensitive to the increase in mass flow rate ratio (mw/ma). This was confirmed by a study carried out by Masoud Khorasani [13] using a humidifier operating on the principle of an airlift pump. The studies achieved by Rodica Borcial [14] and Parviz Enavy [15] showed that the air flow is forced which will lead to the circulation of water. The results obtained are comparable to those obtained by Z. Rahimi Ahar and Mohamed Asa [11, 12].

The main objective of this paper is the numerical and experimental investigation of the main parameters of a new Humidification-dehumidification desalination (HDD) process operating on the principle of an airlift pump where air and water are in upward flow. The packed column has a variable height depending on the desired productivity of distilled water. The brine coming out of the evaporator is hot water is recycled, through a down comer, to humidify new air stream. This new system is characterized by the absence of flooding whatever the value of (mw/ma). In addition, its configuration is a favorable condition for the evaporation of water in contact with air. The numerical and experimental works studied the influence of the operating conditions such as water temperature, the submerged ratio and the air flow rate on the air temperature and humidity profiles.

2. Research Significance

The lack of fresh water in the world and the growing need for distilled water have pushed researchers to design and carry out water desalination processes. Air humidification and dehumidification is one of the processes used in small to medium water desalination units. The size of these units depends, among other things, on the operating conditions and the configuration. Therefore, this study focuses on assessing the effects of operating conditions on the temperature and humidity profiles. The results may provide guidance for a multi-criteria optimization of desalination units by HDD.

3. System Description

3.1. Experimental Setup

Figure 1 illustrates a schematic diagram. The experiments were performed on a vertical cylindrical column made up in three glass tubes 0.072 m diameter and 0.4 m length. The total height of the column and the packed bed are 1.2 m and 1.0 m respectively. The characteristics of the solid packing are shown in Table 1. The column is provided with equidistant pressure sensors in order to measure the local pressure at different heights. Four polypropylene disc diffusers, with 67 circular pores of 5 mm each, are arranged at the ends of the glass tubes. They have a double role: first they change the fluid flow direction, second they prevent the exit of solid packing out of tube. Only one air jet nozzle used in the experiments. It has a diameter of 3 mm.

At the input of the column, a swirl chamber, stainless steel, is designed for the injection of water and air. At a height equal to 1.02 m of the column, water is recycled through a down comer and the air continues the path to the cyclone and condensers.

Water droplets separated at the cyclone are routed to the swirl chamber. A make-up tank of water (7) is placed to keep a constant liquid level in the down comer. The compressor used of 2 kW power, Michelin type and 25 liters of tank, provided with a flow controller valve.

The air flow meter is air float type; brand Tubux whose measuring range is between 0 and 25 m^3/h and the uncertainty of 4%. The setup is designed in a manner that the amount of water evaporated will be replaced, automatically, by the same amount of liquid brackish water issued from the tank (7) which has a controlled level. The riser is used as an evaporator chamber. It is insulated by a transparent polyethylene layers. The liquid supply and outlet flow rates are regulated by valves so as to keep a constant submersion ratio.

The airflow humidified by passing through water level in evaporator chamber then leaves from the outlet pipe in the direction of condensers. The water level in the evaporator chamber is controlled by the level of water make up tank (7) and an electric heater (3) of 2 kW power. The inlet water flow rate in the evaporator is measured by a calibrated orifice (6).

Table 1. *Physical characteristics of the packing.*

Type of solid	Glass rings
Density: ρ_S	2.187 (kg/m^3)
Average diameter: d_p	0.008 (m)
Average length: l_p	0.008 (m)
Fixed bed porosity: ε	77.3
Form Factor: φ_p	0.681

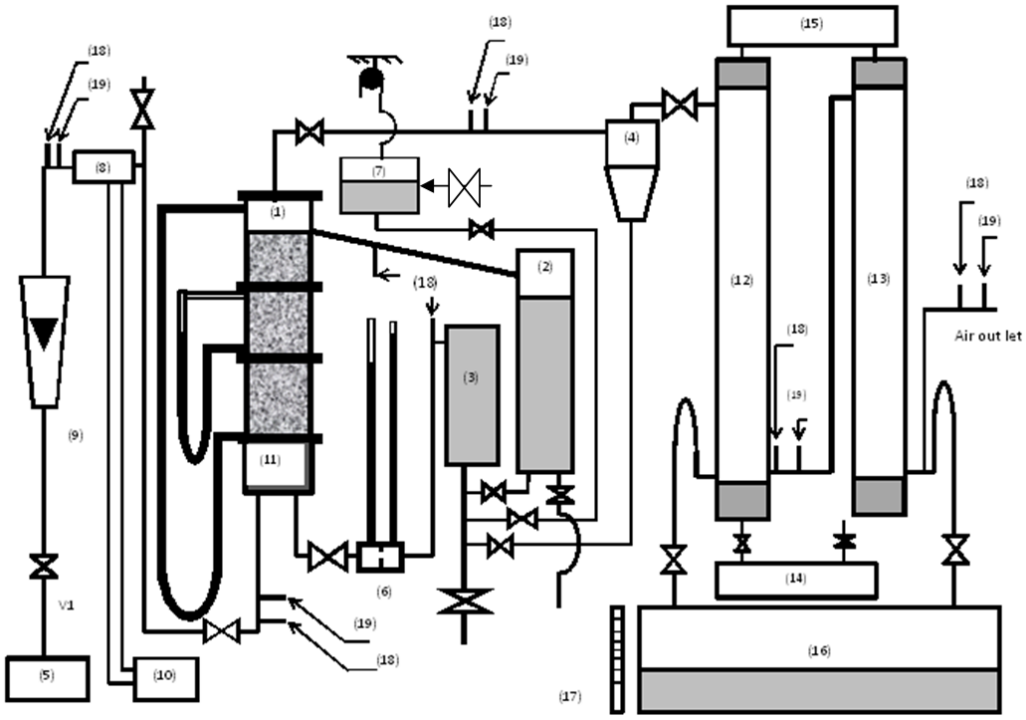

a) Schematic diagram

b) Real image of the setup

Figure 1. *Schematic diagram and real image of the experimental setup.*

3.2. Airlift Pump System

The air lift system is composed with a submerged vertical tube, filled with packing, in which air coming from a compressor is injected at the base. As a result of the gas bubbles suspended in the fluid the average density of the two-phase fluid mixture is less than that of the surrounding liquid. The resulting buoyant force causes a pumping action. The water pumped with air lift depends on the air flow rate and submersion ratio, S. The submersion ratio is defined as the ratio Zs/Zt, where Zs and Zt are the initial height of water in the vertical tube and the total height of the column respectively. The pumping performances of the air lift pump in ordinary conditions are performed by A. Oueslati et al [3]. The height of the packed column is adjustable by adding or removing of glass tubes of diameter 0.072 and 0.4m length to the riser. It depends on the looked efficiency of the system.

4. Formulation Problem

4.1. Mass Balance

Consider a phase made up of two constituents, liquid: water (1) and gas: hot air (2). Consider the volume element of the packed column. The overall steady-state water mass balance is written as follows:

$$(m_{L1} - m_{L2}) = m_G(X_2 - X_1) \quad (1)$$

Differential material balance on the volume element dV:

$$m_G.dX = -dm_L \quad (2)$$

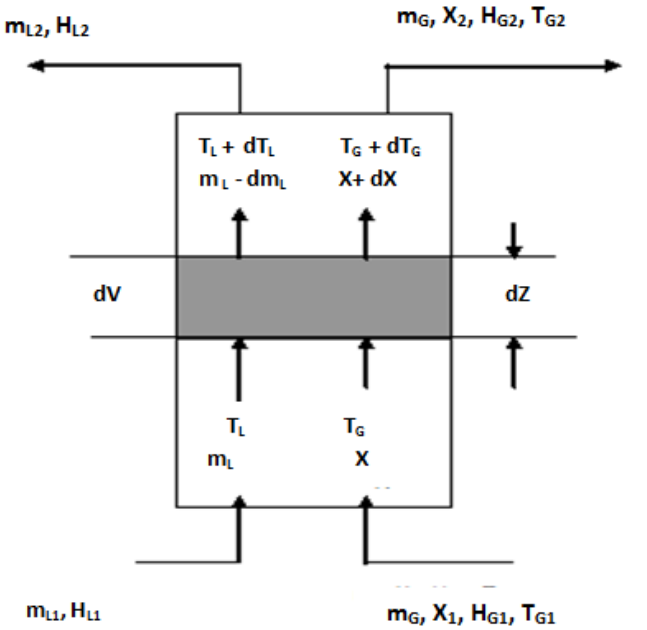

Figure 2. *Material and energy balance on an element of the evaporator volume.*

4.2. Energy Balance

The contactor is assumed to be adiabatic, so there is no input or loss of heat, so the overall balance on the volume element dV is:

$$m_{L1}.H_{L1} + m_G.H_{G1} = m_G.H_{G2} + m_{L2}.H_{L2} \quad (3)$$

With:

$$H_{G1} = (C_A + X_1.C_V).(T_1 - T_0) + \lambda_0 * X_1 \quad (4)$$

$$H_{G2} = (C_A + X_2.C_V).(T_2 - T_0) + \lambda_0 * X_2 \quad (5)$$

We pose:

$$C_S = (C_A + X.C_V) \quad (6)$$

Differential energy balance on the volume element dV:

$$m_G.dH_G = d(m_L.H_L) \quad (7)$$

Now the term:

$$d(m_L H_L) = m_L dH_L + H_L dm_L = m_L C_L dT_L + H_L dm_L \quad (8)$$

With:

$$H_L = C_L(T_L - T_0) \quad (9)$$

It is assumed that the average heat capacity of the liquid, CL, is constant. We take the reference temperature: $T_0 = 0°C$. So:

$$H_L = C_L T_L \quad (10)$$

So equation (8) is written as:

$$d(m_L H_L) = m_L dH_L + H_L dm_L = m_L C_L dT_L + C_L T_L dm_L \quad (11)$$

The combination of equations (7), (8), (9), (10) and (11) gives:

$$m_G dH_G = m_L C_L dT_L + C_L T_L dm_L \quad (12)$$

The term $m_G\ dH_G$ can be developed as follows:

$$m_G dH_G = m_G * d[(C_A + X.C_V) * (T_G - T_0) + X.\lambda_0] \quad (13)$$

Is:

$$m_G * dH_G = m_G * \left[C_A dT_G + (T_G - T_0).C_v.dX + X.C_v.dT_G + \lambda_0.dX\right] \quad (14)$$

From where:

$$m_G * dH_G = m_G[(C_A + X.C_v)dT_G + (C_v.T_G + \lambda_0)dX] \quad (15)$$

We take into account the heat transfer in the liquid film:

$$d(m_L * H_L) = h_L * a_H * (T_L - T_i) * dz \quad (16)$$

With: h_L, Heat exchange coefficient by convection in the liquid film,a_H, Heat exchange area, T_i, Temperature at the liquid gas interface, T_L: Temperature in the core of the liquid phase.

For the gas (Air)

The term sensible heat is written:

$$m_G(C_A + X.C_v)dT_G = h_c * a_H * (T_G - T_i) * dz \quad (17)$$

Is:

$$\frac{dT_G}{dz} = \frac{h_c * a_H}{m_G * (C_A + X.C_v)}(T_G - T_i) \quad (18)$$

h_c, Coefficient of heat transfer by convection in the gas film, T_i, temperature at the liquid - gas interface and T_G, air Temperature.

The term evaporation is:

$$m_G * \lambda_0 * dX = \lambda_0 * N_A * a_M * dz \quad (19)$$

N_A, Mass density of material transfer from the liquid phase to the gas phase.

$$N_A = K_X * (X_i - X) \quad (20)$$

K_X: Coefficient of material transfer in the gas film, X_i, X: Absolute humidity at the interface and in the heart of the gas phase. The combination of equations (19) and (20) gives:

$$m_G * dX = K_X * (X_i - X)\, a_M * dz \quad (21)$$

$$\text{Is: } \frac{dX}{dz} = \frac{K_X a_M}{m_G}(X_i - X) \quad (22)$$

Combining equations (15) - (22), let us write:

$$m_G\, dH_G = h_c\, a_H\, (T_G - T_i)\, dz + \lambda_0\, K_X\, (X_i - X)\, a_M\, dz \quad (23)$$

We use LEWIS number:

$$Le = h_C / K_X * (C_A + X.C_v) = h_C / K_X.C_S \quad (24)$$

suppose:

$$a_H = a_M = a \quad (25)$$

So equation (23) becomes:

$$m_G.dH_G = K_x.a.\left[\frac{h_C}{K_x} * (T_G - T_i) + \lambda_0.(X_i - X)\right] * dz \quad (26)$$

Or:

$$h_C \,/\, K_X = Le.C_S \tag{27}$$

Equation (23) becomes so:

$$m_G\, dH_G \;= K_X a\, \left(Le.C_S.(T_G \;-\; T_i\,) \;+\; \lambda_0\,(X_i \,-\, X)\right)\, dz \tag{28}$$

So:

$$m_G\, dH_G \;= K_X a\, [(\lambda_0.X_i - Le.C_S * \;\; T_i) - (\lambda_0.X - Le.C_S * \;\; T_G)]\, dz \tag{29}$$

For the couple water – air, $Le = 1$ [8, 16, 17]. So:

$$m_G \;*\; dH_G \;= K_X \;* a \;* \left[H_i \,-\, H_G\right] * \; dz \tag{30}$$

Is: $\frac{dH_G}{dz} = \frac{K_X.a}{m_G}(H_i - H_G)$ (31)

H_i: enthalpy at the interface, H_G: enthalpy in the gas phase. Let's divide equation (31) by equation (22), we get:

$$\frac{dH_G}{dz} = \frac{(H_i - H_G)}{(X_i - X)} \tag{32}$$

Equation (7) can be written as follows:

$$m_G \;*\; dH_G \;=\; m_L\, C_L\, dT_L \;+\; C_L \;*\; T_L \;*\; dm_L \tag{33}$$

Or:

$$m_G\, dH_G \;-\; C_L\;T_L\, dm_L \;=\; m_L\, C_L\, dT_L \tag{34}$$

The mass balance on water is:

$$m_G\, dX \;= -\, dm_L \tag{35}$$

Replace dm_L by its expression, then:

$$m_G\, dH_G \;-\; C_L\, T_L\, m_G dX \;=\; m_L\, C_L\, dT_L \tag{36}$$

Division equation (36) by (dX), we obtain:

$$\frac{dT_L}{dX} = \frac{m_G.\left(\frac{dH_G}{dX} - C_L.T_L\right)}{m_L.C_L} = \frac{m_G}{m_L.C_L}\left(\frac{dH_G}{dX} - C_L.T_L\right) \tag{37}$$

A material balance between the base of the column and any section, we get:

$$m_L \;=\; m_{L1} \;-\; m_G\,(X \,-\, X_1) \tag{38}$$

Then equation (37) gives:

$$\frac{dT_L}{dX} = \frac{m_G.\left(\frac{dH_G}{dX} - C_L.T_L\right)}{m_L.C_L} = \frac{m_G}{(\,m_{L1} - m_G * (X - X_1)).C_L}\left(\frac{(H_i - H_G)}{(X_i - X)} - C_L.T_L\right) \tag{39}$$

After rearrangement, we will have:

$$\frac{dT_L}{dX} = \frac{m_G.\left(\frac{dH_G}{dX} - C_L.T_L\right)}{m_L.C_L} = \frac{1}{\left(\frac{m_{L1}}{m_G} - (X - X_1)\right).C_L}\left(\frac{(H_i - H_G)}{(X_i - X)} - C_L.T_L\right) \tag{40}$$

Dividing equation (18) by equation (22), we get:

$$\frac{dT_G}{dX} = \left(\frac{h_C}{K_X.C_S}\right)\frac{T_G - T_i}{X - X_i} \tag{41}$$

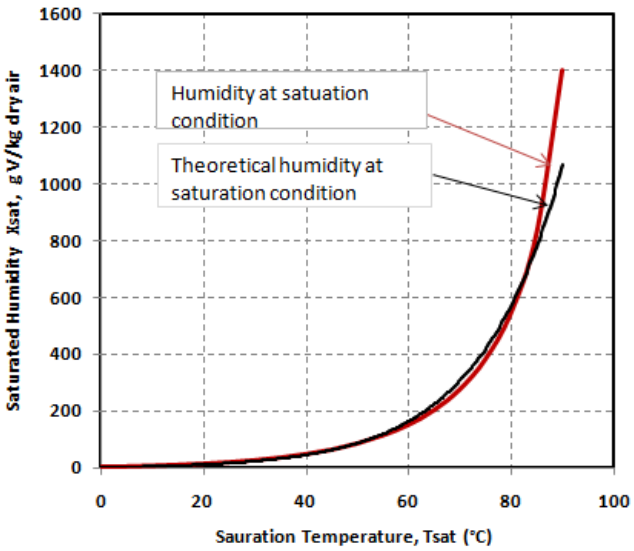

Figure 3. *Absolute and theoretical Humidity at saturation conditions versus saturation temperature.*

The conditions at the interface are those at saturation. Figure 3 shows the evolution of humidity ratio versus temperature under atmospheric conditions. The data are taken from reference [3]. From this figure, we see that humidity ratio increases with the increase of temperature. Data modeling has been implemented. The theoretical model is given by the following equation:

$$X_{Sat,Th} = 4.0041 * \exp(0.0621 * T),\ R^2 = 0.9974 \quad (42)$$

5. Solution of the Model Governing Equation

In what follows, we will attempt to plot the temperature, TG, and absolute humidity, X, of the gas. So, the system to be solved consists of equations (18) and (22). To solve this system, we have the boundary conditions at the entry and exit of the column. The data entering the column are: Gas temperature, TG1, absolute gas humidity, X1, dry air flow, mG, Liquid water flow, mL1. The data at the exit of the column are: absolute humidity of the gas, X2, Temperature of the gas and the liquid, TG and TL. We have adopted the following assumptions: The liquid temperature remains unchanged. The temperature at the interface is equal to that of the liquid. The heat exchange air is equal to the matter exchange area. The flow regimes of water and air are turbulent. No radial dispersions of gas temperature and absolute humidity. Air does not dissolve in water. To solve this system of equation, we used the Runge-Kutta method of order 4. The calculation of the parameters starts from the foot towards the head of the column. The overall scheme of the resolution consists of the following steps:

Step 1- Choose a value for each parameter of the operating conditions: submersion ratio, water temperature, temperature and mass flow rate of the gas entering the column.

Step 2- Choose a value for each of the following ratios: $\left(\frac{h_c a_H}{m_G(C_A+X.C_v)}\right)$ et $\left(\frac{K_X\, a_M}{m_G}\right)$.

Step 3- Run the resolution flowchart using the Runge-Kutta method.

Step 4- Compare the values of the temperature and absolute humidity of the gas calculated by the Runge-Kutta method of order 4 with those measured at the head of the column. If the calculated temperature and humidity and those measured are equal then the values of the ratios chosen are correct. Otherwise, you have to redo the resolution from step 2.

The values of the heat and mass transfer coefficients found during the numerical resolution of the model will be explained and studied in depth in part II of this article.

6. Theoretical and Experimental Results

We followed the resolution path described in the previous paragraph. For each submersion ratio and air flow and water temperature, we determined the air temperature and absolute humidity profiles in the column. The advantage of the resolution procedure lies in the equality of the air characteristics measured at the head of the column with those calculated by the established model.

Table 2. *Operating conditions of the experimental tests.*

S_r	0,4	0,5	0,6	
m_G (kg/h)	1	3	5	
T_w (°C)	40	60	75	85

Each operating condition is defined by unique values for mG, Sr and Tw. From this table, we have a total of 36 operating conditions. The curves giving the profiles of the air temperature and the absolute humidity in the packed column relating to the operating conditions are shown in the following table:

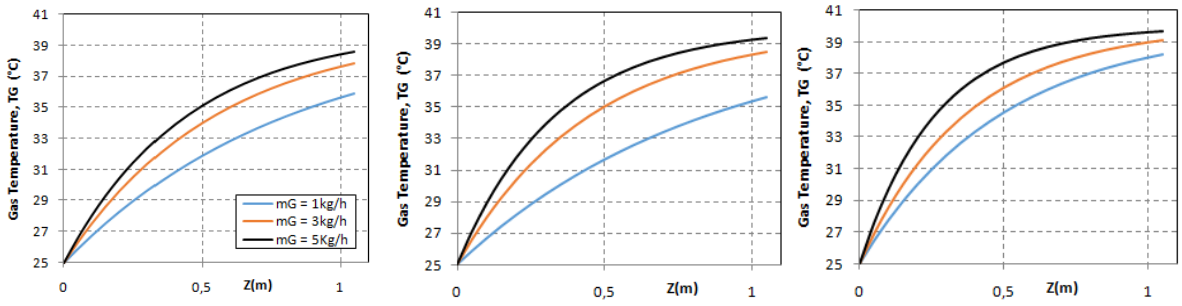

a1) Sr = 0.4; Tw= 40°C b1) Sr = 0.5; Tw=40°C c1) Sr=0.6; Tw=40°C

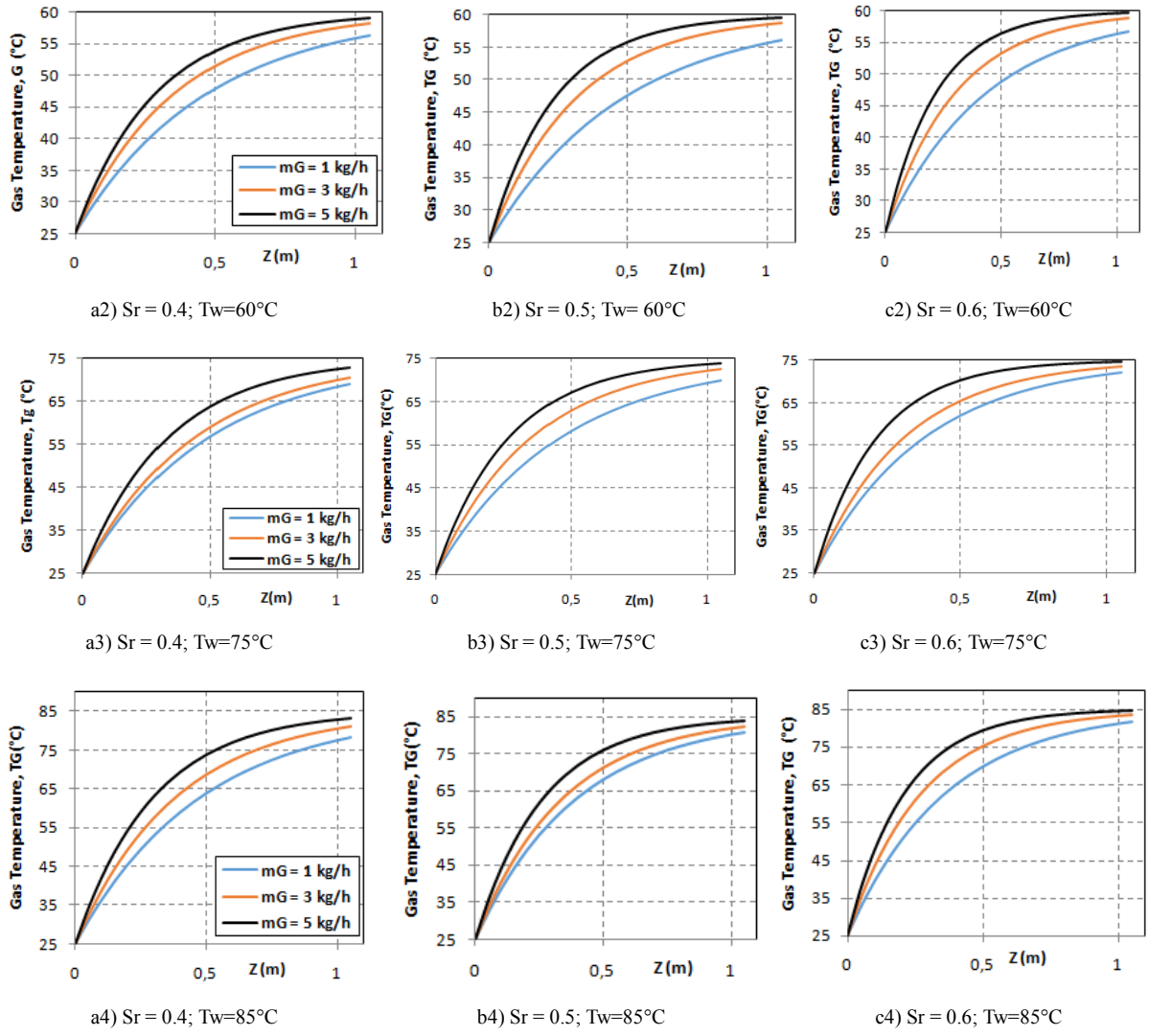

a2) Sr = 0.4; Tw=60°C b2) Sr = 0.5; Tw= 60°C c2) Sr = 0.6; Tw=60°C

a3) Sr = 0.4; Tw=75°C b3) Sr = 0.5; Tw=75°C c3) Sr = 0.6; Tw=75°C

a4) Sr = 0.4; Tw=85°C b4) Sr = 0.5; Tw=85°C c4) Sr = 0.6; Tw=85°C

Figure 4. *Numerical values of gas temperature versus packed column height.*

Figure 4 shows the theoretical results of the evolution of the gas temperature as a function of the packing height under different operating conditions. These operating conditions are defined by the water temperature of 40°C to 85°C, the submersion ratio of 0.4 to 0.6, and the air mass flow rate of 1 to 5 kg/h. From this figure, we see increasing curves and the majority of heat transfers are carried out in the first half of the column.

Table 3. *Difference between the numerical value and the experimental value of the air temperature at the outlet of the column.*

Tw	**°C**	**40**			***60***			**75**			**85**		
mG	**kg/h**	**1**	**3**	**5**	**1**	**3**	**5**	**1**	**3**	**5**	**1**	**3**	**5**
Sr		0.4											
T exp	°C	35	37.,5	38,5	55	58	59	68,5	70	72,5	78	81	83
T cal	°C	35.9	37.81	38,59	56,24	58,22	59,12	69,14	70,5	72,87	78,31	81,1	83,24
ε_T	%	2.,55	0.82	0,25	2,21	0,4	0,2	0,93	0,68	0,5	0,4	0,13	0,29
Sr		0.5											
T exp	°C	35,5	38,5	39,5	55,8	58,5	59,5	70	72	74	80,5	82	83,7
T cal	°C	35,65	38,54	39,35	56,08	58,82	59,61	70,04	72,48	74,01	80,82	82,27	83,89
ε_T	%	0,44	0,12	0,37	0,51	0,54	0,2	0,06	0,67	0,023	0,4	0,33	0,23
Sr		0.6											
T exp	°C	38	39,1	39,7	56,5	58,9	59,7	71,8	73,4	74,6	81,5	83,7	84,5
T cal	°C	38,21	39,13	39,718	56,83	58,91	59,708	72,04	73,44	74,65	81,63	83,72	84,58
ε_T	%	0,57	0,07	0,047	0,58	0,03	0,015	0,34	0,065	0,07	0,16	0,03	0,1

Table 3 represents the theoretical, Tcal, and experimental values, Texp, of the temperature of the outlet of the humidifier as well as the relative deviation, ε_T, between them. Note that the relative deviation is less than 3% which proves

the validity of the established theoretical model.

6.1. Air Temperature Variation TG

6.1.1. Effect of Submersion Ratio (Sr) on Temperature TG

The submersion ratio has an effect on the pumped water flow rate [14, 15]. According to a previous study, the flow of water, circulated, is proportional to the liquid temperature. It is above 200 kg / h for submersion ratios greater than 0.35 [14]. Figure 5 shows the evolution outlet gas temperature versus submersion ratio under constant water temperature, Tw, and constant air flow rate, mw. From this figure, we see that the submersion ratio has a small effect. Indeed, the increase of outlet gas temperature is less than 3% when the submersion ratio varies from 0.4 to 0.6.

6.1.2. Effect of Water Temperature on Gas Temperature TG

The water temperature is a main parameter in airlift systems since it actively contributes in pumping water [13-15]. From which the air is brought into contact with a large flow of hot water in a packed column which promotes the transfer of heat between the two fluids. Figure 6 shows the evolution of outlet gas temperature versus water temperature under constant submersion ratio, sr, and constant air flow rate, ma. From this figure, we see that the outlet gas temperature is influenced strongly by that of water.

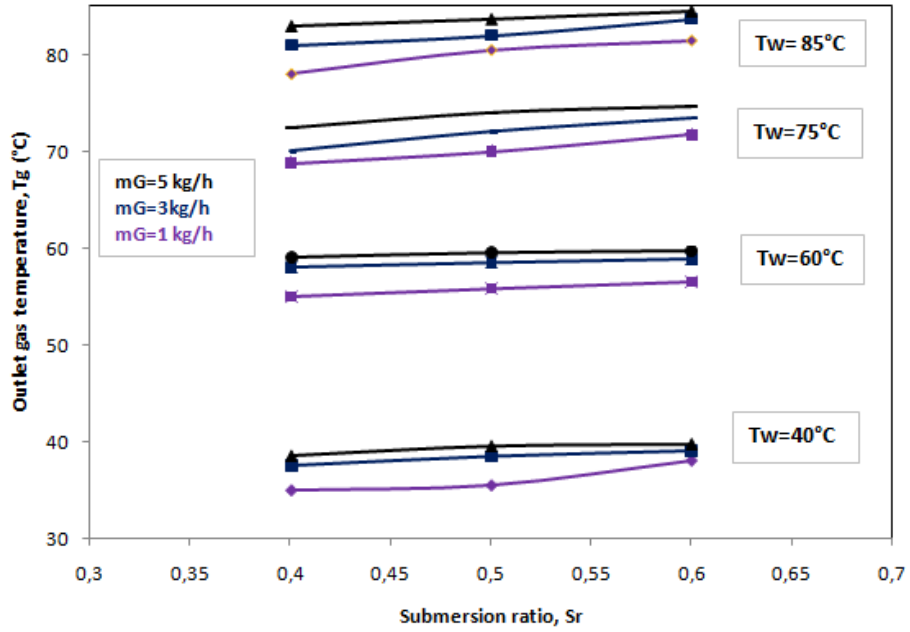

Figure 5. *Effect of submersion ration on outlet gas temperature.*

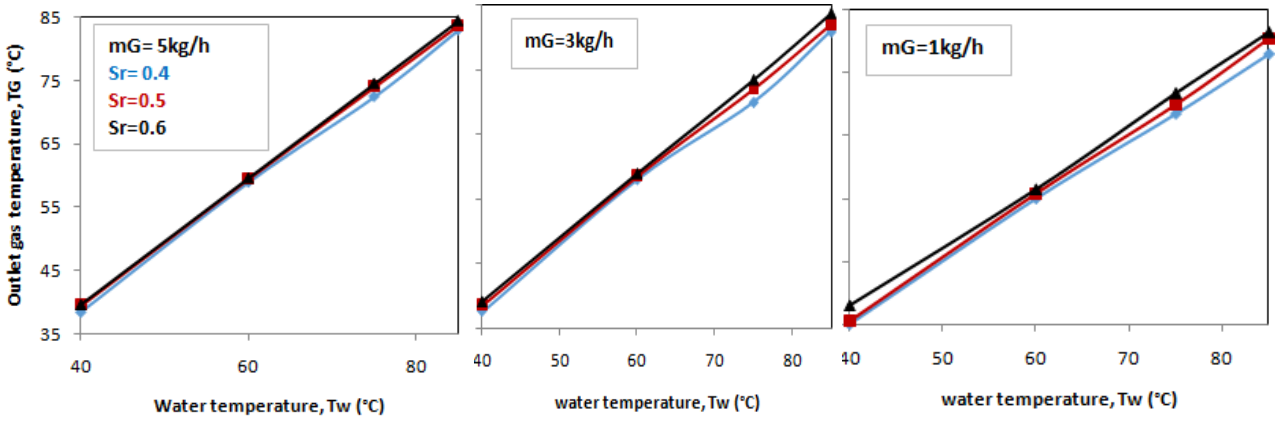

Figure 6. *Effect of water temperature on outlet gas flow rate temperature.*

6.1.3. Effect of Air Flow Rate on Gas Temperature TG

Figure 7 shows the evolution of outlet air temperature versus air flow rate under constant water temperature and constant submersion ratio. From this figure, we see that the greater the air flow, the closer the outlet air temperature is to that of liquid water.

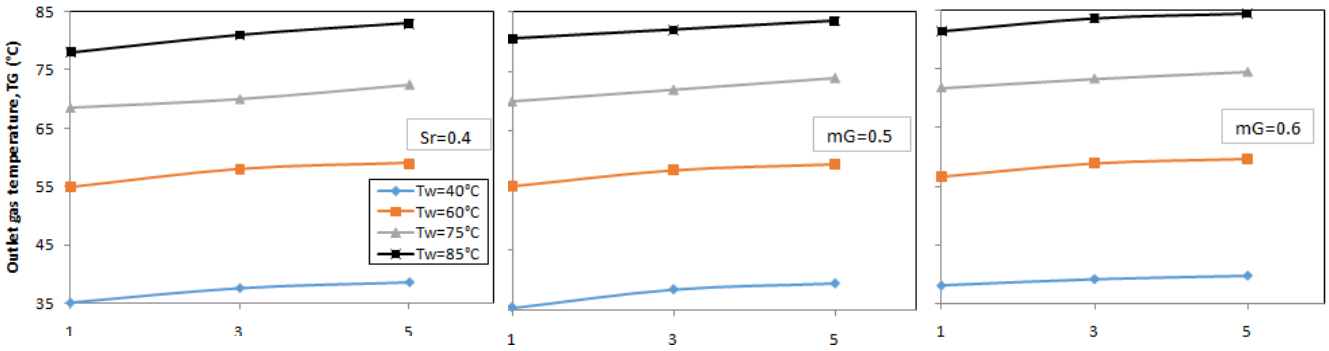

Figure 7. *Effect of air flow rate on outlet gas temperature.*

6.2. Change in Absolute Humidity X

The numerical results of absolute humidity versus packed column height, under different operating conditions, are illustrated in figure 8. each operating condition is defined by a submersion ratio, water temperature and air flow rate. From this figure, we see increasing curves, and the maximum mass transfer took place in the first half of the humidifier column whatever the operating conditions.

Table 4. *Difference between the numerical values and the experimental values of the absolute humidity at the outlet of the column.*

Tw	**40**			**60**			**75**			**85**		
mG	**1**	**3**	**5**	**1**	**3**	**5**	**1**	**3**	**5**	**1**	**3**	**5**
Sr	0.4											
X exp	0,035	0,039	0,048	0,135	0,15	0,152	0,36	0,37	0,385	0,792	0,8	0,83
X cal	0,03526	0,03938	0,049	0,138	0,1506	0,1533	0,3626	0,3718	0,3856	0,794	0,801	0,8319
ε_X	0,74	0,98	2,18	2,12	0,4	0,9	0,73	0,5	0,16	0,26	0,2	0,23
Sr	0.5											
X exp	0,038	0,04	0,0492	0,141	0,153	0,159	0,367	0,375	0,395	0,798	0,812	0,839
X cal	0,0381	0,0404	0,0493	0,1414	0,1533	0,1598	0,3682	0,3765	0,397	0,802	0,8136	0,8398
ε_X	0,02	1,19	0,23	0,32	0,24	0,53	0,33	0,42	0,43	0,6	0,2	0,1
Sr	0.6											
X exp	0,0385	0,0415	0,0496	0,149	0,158	0,168	0,377	0,385	0,415	0,8	0,818	0,847
X cal	0,03875	0,04151	0,04987	0,1492	0,1584	0,1681	0,3771	3856	0,4165	0,804	0,819	0,851
ε_X	0,64	0,001	0,55	0,14	0,27	0,08	0,04	0,16	0,37	0,5	0,12	0,54

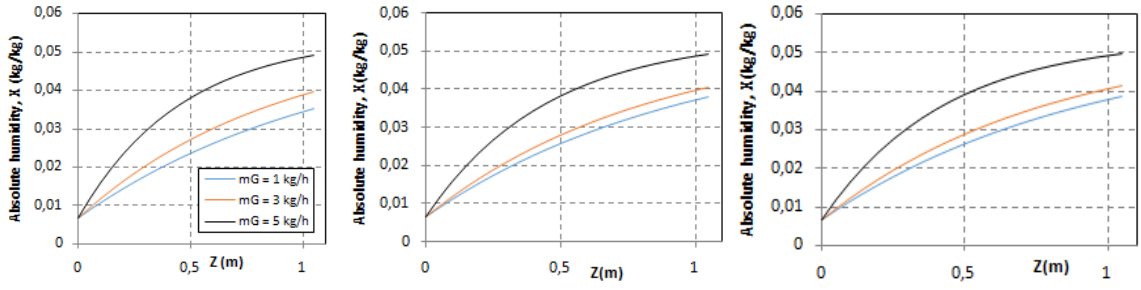

a1) Sr= 0.4; Tw=40°C b1) Sr = 0.5; Tw=40°C c1) Sr = 0.6; Tw=40°C

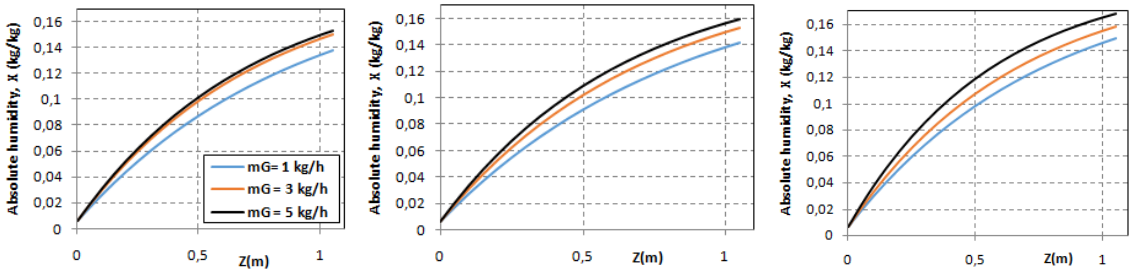

a2) Sr=0.4; Tw=60°C b2) Sr=0.5; Tw=60°C c2) Sr=0.6; Tw=60°C

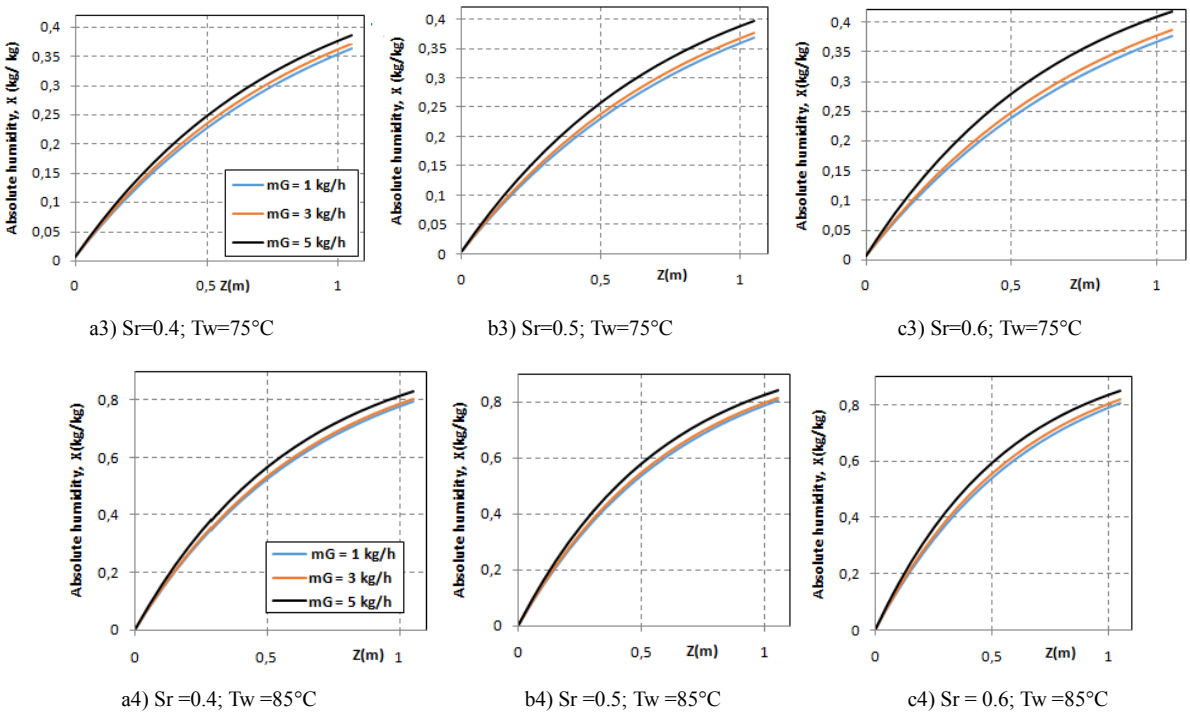

a3) Sr=0.4; Tw=75°C b3) Sr=0.5; Tw=75°C c3) Sr=0.6; Tw=75°C

a4) Sr =0.4; Tw =85°C b4) Sr =0.5; Tw =85°C c4) Sr = 0.6; Tw =85°C

Figure 8. *Numerical values of absolute humidity versus packed column height in different conditions.*

Table 4 mainly shows the relative difference between the value calculated by the numerical model and that obtained experimentally. The relative deviation is less than 2% which confirms the validity of the model obtained.

6.2.1. Effect of Submersion Ratio (Sr) on the Absolute Humidity X

Figure 9 shows the evolution of outlet absolute humidity versus submersion ratio under the conditions of constant water temperature and constant air flow rate. From this figure, we see slightly increasing curves. which proves a weak effect of submersion ratio on absolute humidity. Indeed, the variation in absolute humidity versus the variation in the submersion ratio is always less than 3%.

6.2.2. Effect of Water Temperature on the Absolute Humidity X

Figure 10 shows the evolution of outlet absolute humidity versus water temperature under constant air flow rate and constant submersion ratio. From this figure, we see the strong effect on the outlet humidity ratio. Above 60°C, the increase in absolute humidity, depending on the temperature of the liquid water, becomes almost exponential.

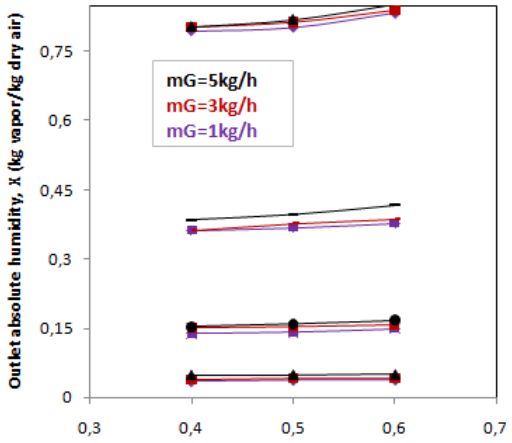

Figure 9. *Effect of submersion ratio on the humidity profile.*

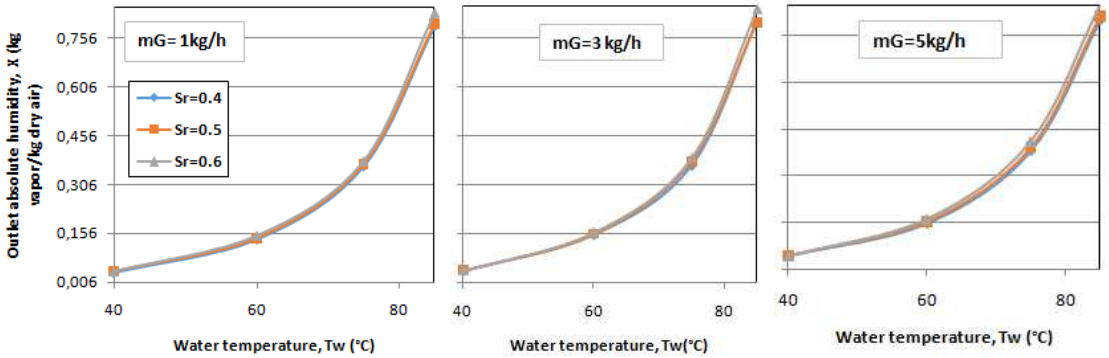

Figure 10. *Effect of water temperature on the absolute humidity.*

6.2.3. Effect of Air Flow on Absolute Humidity X

Figure 11 shows the evolution of outlet absolute humidity versus air flow rate. From this figure we observe that effect of air flow rate on outlet absolute humidity exists but not very high.

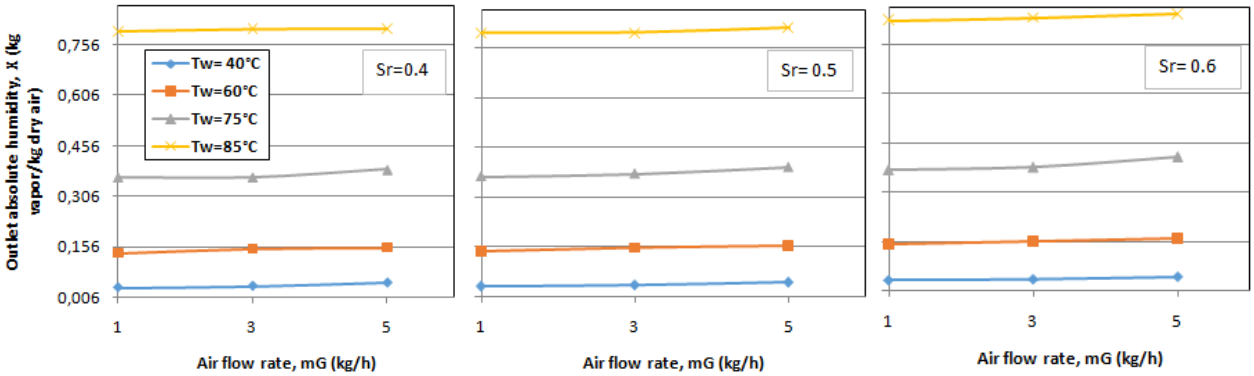

Figure 11. *Effect of the air flow rate on the humidity profile.*

7. Comparison of the Present Results with Those in Literature

Figure 12 shows the evolution of outlet air temperature versus water temperature obtained by various authors. A comparison between the values obtained in this study with those obtained by other authors is achieved. From this figure, we observe that the values obtained in this study are close to those obtained by Adel Ben Lakhdhar Oueslati and Adel Megriche [3] when the water temperature is lower than 55°C.

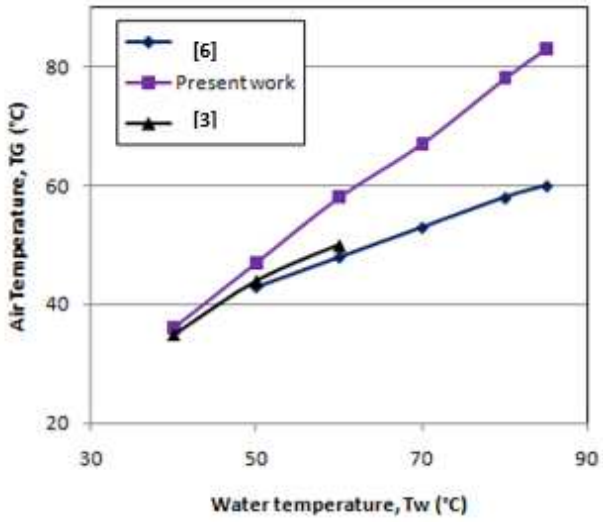

Figure 12. *Comparison of outlet air temperature values with that in literature.*

Figure 13 shows the evolution of outlet humidity ratio at the outlet of the humidifier as a function of the water temperature obtained by various authors. A comparison between the values obtained in this study with those obtained by other authors is achieved. From this Figure, we see that the values obtained in this study are close to those obtained by Z. Rahimi [11]. The results obtained by Xin Huang and Salman H. [6, 18] are modest by comparison with those obtained in this study.

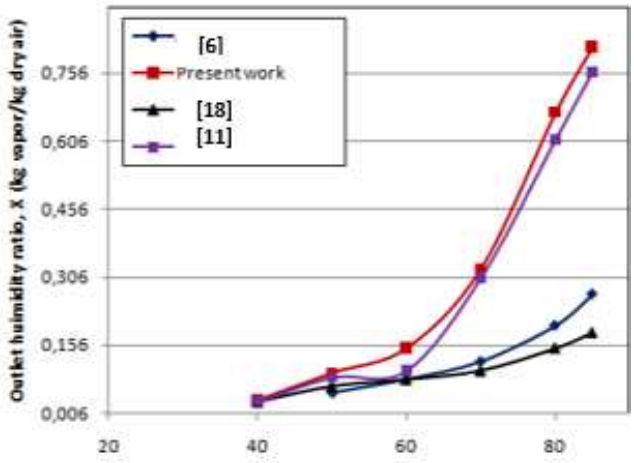

Figure 13. *Comparison of outlet humidity ratio values with that in literature.*

Examination of the work of several authors researches on cooling towers such as A. Zargar [8], ACB Thomé [9] and SK Ziganshina [17] shows that the countercurrent flow of water and air in a packed column is accompanied by low humidification air. This is explained by the low temperature levels of water and air. However, the counter-current flow of fluids is an unfavorable condition for the evaporation of water in the air whatever the value of the flow rate ratio of the fluids (mw/ma).

8. Discussion

For more than twenty century, contact air-water processes have been the subject of investigation. This contact is used either to cool the water using an ascending cold air flow in a cooling tower [8, 9, 17] or for the production of distilled water by humidification-dehumidification desalination process [1-7, 10-15].

A review of the open literature has shown that humidification techniques by spraying water into air have

modest performance [4, 5] even when multiple stages of HDD are used. High performance HDD systems are classified into three classes:

HDD systems with a packed column as humidifier, but water and air flow vertically in opposite directions [2, 3, 6]. These systems are similar to cooling towers [8, 9, 17]. The maximum absolute humidity at the outlet of the humidifier is obtained when the water temperature is high.

The second class of HDD systems are characterized by a humidifier where the water is almost stagnant, crossed by air bubbles which become humidified by contact. These systems are studied by [10-12]. It has been shown that the presence of a condenser has a direct effect on the rate of humidification of the air in the humidifier. The results presented by [10-12] prove that the maximum humidity at the outlet of the humidifier, in contact with the free air, is less than 240 g v / kg dry air. But, if the humidifier is connected to a condenser, then the humidity at the output of the humidifier is around 0.8 kg v / kg dry air.

The third class of HDD systems with a packed column, but the flow of water and air is upward. So, the air humidification rate is comparable with those obtained in class 2 [13-15]. The difference in performance between the three classes is explained by the pressure of the liquid on the air. In fact, in the first class, the descending water exerts a static pressure and a dynamic pressure proportional to the square of its flow rate on the ascending air. This pressure can reach a value where the air is braked and it cannot reach the head of the column. This condition is not favorable to the evaporation of water. Therefore, this configuration is used, mainly, in cooling towers with negligible loss of water by evaporation [8, 9, 17].

While, in HDD systems with nearly stagnant water, the air is subjected to static water pressure. The dynamic pressure is negligible since the speed of the liquid is low. This condition is favorable to the evaporation of water since the duration of contact between the fluids is sufficient for the exchanges of heat and matter.

For co-upflow HDD systems and more specifically airlift systems were introduced in 2014 [13-15]. The air humidification rate is high since the dynamic pressure of the liquid is suppressed. The presence of condenser has a beneficial effect on humidification.

The study of the humidification simulation showed that the operating parameters such as the submersion ratio, the temperature of the liquid water, the gas flow rate and the variable height of the column. Indeed, for high temperatures above 85°C, the submersion ratio must be low and it must not exceed the value 0.4 because the high amount of evaporated water creates high air pressure and fluid speeds. become very fast [14, 15]. Under the operating conditions tested, the majority of the quantities of heat and material exchange is carried out in a packing height of 50 cm.

More fundamental and experimental explanations on liquid-gas contactors as well as recommendations on the relationship between operating conditions and performance of cooling towers and humidifiers will be presented in an upcoming article.

9. Conclusion

In this study, we modeled the heat and material transfers between water and air in a flow, of the air lift type, in a packed column. We obtained the profiles of the air temperature and the absolute humidity at any given height point. The difference between the values calculated by the model and those obtained by the experiment is less than 3%. As a result, the established model validity was confirmed. The conclusions emanating from this experimental and numerical investigation can be drawn as follows:

1. The effect of raw water temperature on air temperature and absolute air humidity at outlet is greater than that of air flow rate and submersion ratio.
2. The ascending co-current flow, of airlift type, of liquid and gas in a packed column is a favorable condition for the humidification of the air thanks to the low dynamic pressure exerted on the water molecules.
3. Airlift systems used for air humidification are more efficient than air humidification systems where fluids are in counter-current flow. In addition, unlike other air humidification systems, air lift systems are not sensitive to the ratio of mass flow rates of fluids (mw/ma). No risk of flooding whatever the value of the ratio of mass flow.
4. Countercurrent air-water contactors are effectively used as cooling towers, instead of using them as air humidification systems, because of the low evaporation of water under the effect of great dynamic pressure.
5. Air lift humidifiers are effective when the raw water temperature is high. A height of 1 m of the packed column, in the assembly configuration used, is sufficient to achieve absolute humidity values close to that of saturation.

Nomenclature

Parameter	Definition
A	Air
A	Exchange area
C	Calorific capacity
Cal	Calculated
D	Diameter
Exp	Experimental
G	Gas
H	Enthalpy
H	Height
Hc	Heat transfer coefficient
I	Interface
Kx	Mass transfer coefficient
L	Liquid
L	Length

Parameter	Definition
Le	Lewis number
M	Matter
M	Mass flow rate
N	Mass transfer density
O	Reference conditions
P	Particle
R	Ratio
S	Solid
S	Saturated gas
Sr	Submersion ratio
T	Temperature
T	Total
V	Vapor
W	Water
Z	Height
1	Inlet
2	Outlet
Λ	Latent heat
P	Density
E	Porosity
E	Relative error
Ψ	Form factor

References

[1] He Weifeng, Lu Yu, An Haohao. Parametric analysis of humidification dehumidification desalination driven by photovoltaic/thermal (PV/T) system. Energy Conversion and Management 259 (4): 115520. May 2022. DOI: 10.1016/j.enconman.2022.115520.

[2] Faissal Abdel-Hady ET AL. Simulation and optimization study of the humidification–dehumidification desalination process. Desalination and Water Treatment. doi: 10.5004/dwt.2019.23476.

[3] Adel Ben Lakhdhar Oueslati, Adel Megriche. Air Humidification By Contact With Geothermal Water In Packed Column Humidifier: A Theoretical And Experimental Study. Exploratory Materials Science Research. DOI: 10.47204/EMSR.2.2.2021.157-164.

[4] Xinyi Zhou. On the dimensional analysis for solar desalination using humidification-dehumidification processes. Energy Conversion and Management 244 (7-8): 114595. DOI: 10.1016/j.enconman.2021.114595.

[5] Alsehli, M. A New Approach to Solar Desalination Using A Humidification–Dehumidification Process for Remote Areas. Processes 2021, 9, 1120. https://doi.org/10.3390/pr9071120.

[6] Xin Huang, Tingfen Ke, Yang Li, Xiang Ling. Experimental investigation and optimization of total energy consumption in humidification-dehumidification system. Energy Procedia 158: 3488-3493. February 2019. DOI: 10.1016/j.egypro.2019.01.922.

[7] T. M. Khass, R. H Mohammed, N. A. A. Qasem and S. M. Zubair. Different configurations of humidification-dehumidification desalination systems: Thermal and economic assessment. Energy Conversion and Management 258: 115470. DOI: 10.1016/j.enconman.2022.115470.

[8] A. Zargar, A. Kodkani, A. Peris. Numerical analysis of a counter-flow wet cooling tower and its plume. International Journal of Thermofluids 14 (4): 100139. DOI: 10.1016/j.ijft.2022.100139.

[9] A. C. B. Thomé, P. G. Santos, A. G. Fisch, Using rainwater in cooling towers: Design and performance analysis for a petrochemical company. Journal of Cleaner Production. DOI: 10.1016/j.jclepro.2019.03.249.

[10] E. S. Elagouz, M. M. Abugderah, A. Muhra. Enhanced Performance of Desalination by Air Passing Through Saline Water Using Humidification and Dehumidification Process (Dept. M). DOI: 10.21608/bfemu.2020.126000.

[11] Z. Rahimi-Ahar, M. S. Hatamipour, L. R. Ahar. Air Humidification-Dehumidification Process for Desalination: A review. Progress in Energy and Combustion Science 80: 100850. DOI: 10.1016/j.pecs.2020.100850.

[12] Mohamed ASA, Ahmed MS, Maghrabie HM, Shahdy AG. Desalination process using humidification– dehumidification technique: A detailed review. Int J Energy Res. 2020; 1–52. https://doi.org/10.1002/ er.6111.

[13] Masoud Khorasani, Morteza Zivdar, Farshad Fashchi Tabrizi, Zahra Askari, Kaveh Ostad-Ali-Askari. Measurement of Gas-Phase Mass Transfer Coefficients in a Humidification Column through Random Packing. American Journal of Engineering and Applied Sciences 12 (3): 352-358. DOI: 10.3844/ajeassp.2019.352.358.

[14] Rodica Borcia and Michael Bestehorn. Liquid pumping induced by transverse forced vibrations of an elastic beam: A lubrication approach. PHYSICAL REVIEW FLUIDS 3, 084202 (2018). DOI: 10.1103/PhysRevFluids.3.084202.

[15] Parviz Enany • Oleksandr Shevchenko • Carsten Drebenstedt. Experimental Evaluation of Airlift Performance for Vertical Pumping of Water in Underground Mines. Mine Water and the Environment. DOI: 10.1007/s10230-021-00807-w.

[16] Catrawedarma, Deendarlianto Aan, Indarto Indarto. Statistical Characterization of Flow Structure of Air–water Two-phase Flow in Airlift Pump–Bubble Generator System. International Journal of Multiphase Flow 138: 103596. DOI: 10.1016/j.ijmultiphaseflow.2021.103596.

[17] S. K. Ziganshina, A. A. Kudinov. Heat and Mass Transfer of a Gas–Air Mixture in the Stack of an Evaporative Cooling Tower. Journal of Engineering Physics and Thermophysics 95 (3). DOI: 10.1007/s10891-022-02523-w.

[18] Salman H. Hammadi. Theoretical analysis of humidification – dehumidification process in an open type solar desalination system. Case Studies in Thermal Engineering 12 (2018) 843–851.